Available online at www.sciencedirect.com
ScienceDirect
International Journal of Mass Spectrometry 255–256 (2006) 185–194
International Journal of Mass Spectrometry
www.elsevier.com/locate/ijms

Reactivity of self-assembled supramolecular complexes in the gas phase: A supramolecular neighbor group effect

Marianne Engeser[a,*], Alexander Rang[a], Montserrat Ferrer[b], Albert Gutiérrez[b], H. Tarik Baytekin[c], Christoph A. Schalley[c]

[a] *Kekulé-Institut für Organische Chemie und Biochemie der Universität, Gerhard-Domagk-Str. 1, D-53121 Bonn, Germany*
[b] *Departament de Química Inorgànica, Universitat de Barcelona, Martí i Franquès 1-11, 08028 Barcelona, Spain*
[c] *Institut für Chemie und Biochemie—Organische Chemie, Freie Universität Berlin, Takustr. 3, D-14195 Berlin, Germany*

Received 29 November 2005; received in revised form 5 January 2006; accepted 5 January 2006
Available online 7 February 2006

Abstract

Infrared multi-photon dissociation (IRMPD) spectra of mass-selected, self-assembled supramolecular squares and their gas-phase fragments have been recorded in a Fourier-transform ion-cyclotron resonance (FT-ICR) mass spectrometer. The squares have been transferred into the gas phase by electrospray ionization (ESI) under very soft ionization conditions resulting in a series of signals for intact squares in different charge states by stripping off two or more counter ions. The fragmentation patterns of the squares strongly depend on the parent ion's charge state. For species with a lower number of charges, expulsions of edge ligands prevail, whereas charge separation pathways dominate the dissociation pathways of more highly charged species.

Keywords: Electrospray ionization; Infrared multiphoton dissociation; Mass spectrometry; Polynuclear metal complex; Self-assembly

1. Introduction

Self-assembly [1] is an efficient strategy for the synthesis of complex species under thermodynamic control. In particular, transition metals are valuable building blocks, because of the large variety of coordination geometries they offer. The design of metallosupramolecular species [2] through self-assembly has reached a high level of sophistication. However, the coordinative bonds are often rather weak and many of these species are multiply charged. Desolvated ions in the gas phase thus suffer from charge repulsion within the complexes. Consequently, their mass spectrometric analysis [3] is not always straightforward. For their analytical characterization, earlier studies used fast atom bombardment (FAB) [4] and electrospray ionization (ESI) [5]. In most of these studies, the intensities of the ions of intact complexes were however rather low. Coldspray ionization (CSI) [6], a variant of the ESI method, was thus applied in order to increase the abundance of intact ions. The metallosupramolecular complexes are then observed as a distribution of incompletely desolvated, but intact ions in different charge states. One problem associated with the coldspray approach is the usually low intensity of desolvated ions which would be interesting targets for tandem mass spectrometric experiments.

Typical prototypes for metallosupramolecular species are self-assembling squares [7] which consist of bipyridine (bipy) edge ligands and Pt-diphenylphosphinopropane (dppp) complexes at the corners (Scheme 1). Other metal corners can be utilized [8] and the bipyridine ligand can be replaced by a large variety of other bis-pyridine compounds or other analogues thereof. Depending on several factors (length and flexibility of the edge ligand, nature of the ligand and/or metal at the corner, etc.), the squares may exist in equilibrium with triangular analogues [9,10], since the formation of triangles is entropically favored due to the higher number of triangles assembling from a fixed number of subunits. Throughout this work, we denote the triangles built from the same building blocks as the corresponding squares with letters **a** and **b**, i.e., **1b** is the triangle corresponding to square **1a**. Further, an assembly of *n* corner and *m* edge building blocks is denominated as *n*:*m* complex, irrespective of the number of attached counter ions.

* Corresponding author. Tel.: +49 228 732849; fax: +49 228 735683.
E-mail address: mengeser@uni-bonn.de (M. Engeser).

1387-3806/$ – see front matter © 2006 Elsevier B.V. All rights reserved.
doi:10.1016/j.ijms.2006.01.002

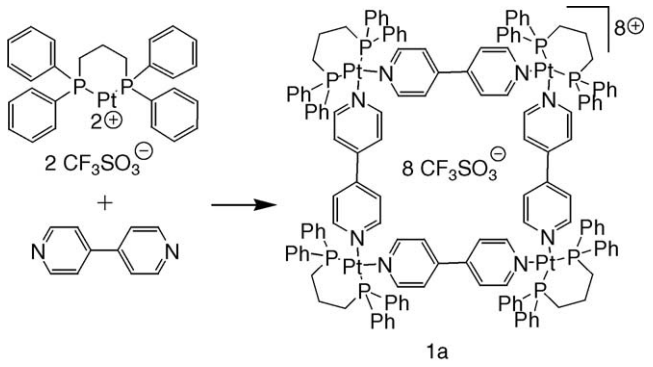

Scheme 1.

In previous publications [11], we have already shown that electrospray ionization under soft ionization conditions can be used to analyze supramolecular squares by tandem mass spectrometry. A detailed fragmentation mechanism for the triply charged square [**1a**–3TfO]$^{3+}$ was deduced involving the supramolecular analogue of a neighbor group effect. In this context it is important to note the difference between gas and condensed phase. Because the metallosupramolecular complexes form under thermodynamic control, they undergo a constant exchange of their subunits in solution. In the gas phase, however, isolated ions are examined and their intrinsic reactivity can be studied without interference of such equilibria. The present article describes a significant improvement of the generation of intact square ions and focuses on the influence of the squares' charge state on the dissociation pathways in the gas phase.

2. Experimental

ESI mass spectra were recorded on a Bruker APEX IV Fourier-transform ion-cyclotron resonance (FT-ICR) mass spectrometer with a 7.05 T magnet and an Apollo ESI ion source equipped with an off-axis 70° spray needle. Typically, acetone solutions of the squares (100–200 μM) were used. Analyte solutions were introduced into the ion source with a syringe pump (Cole-Parmers Instruments, Series 74900) at flow rates of 3–4 μL/min. Ion transfer into the first of three differential pump stages in the ion source occurred through a glass capillary with 0.5 mm inner diameter and nickel coatings at both ends. Ionization parameters were adjusted as follows: capillary voltage, −4.5 kV; end plate voltage, −4.0 kV; capexit voltage, 40–120 V; skimmer voltages, 5 V; temperature of drying gas, 40 °C. Nitrogen was used as nebulizing (25 psi) and drying gas (5 psi). The ions were accumulated in the instruments hexapole for 0.1–1 s, introduced into the FT-ICR cell which was operated at pressures below 10^{-10} mbar and detected by a standard excitation and detection sequence. For each measurement, 16–64 scans were averaged to improve the signal-to-noise ratio. For infrared multi-photon dissociation (IRMPD) experiments, all parameters were adjusted to achieve intense signals for the respective parent ion of interest. Mass-selection of the whole isotopic pattern was followed by irradiation with a CO_2 IR laser at a wavelength of 10.6 μm and a power of maximum 25 W. Although not shown in each case here, a series of measurements with different irradiation times was recorded for every parent ion to monitor the fragmentation kinetics.

3. Results and discussion

It has been shown before that self-assembled supramolecular squares can be detected by ESI mass spectrometry under very soft ionization conditions [11]. Although intact square ions are observed, the spectra are in most cases still dominated by mono- and dinuclear complexes. These fragments may originate from two sources: either they are already present in solution or they are formed during the ESI process, for example due to collisional activation in the ion source region and in the instruments hexapole. Careful adjustment of the ionization parameters, in particular lowering the hexapole accumulation times, increases the abundance of intact ions. Almost fragment-free spectra of **1a** were however obtained only when rather high concentrations of squares in the 100–200 μM range were present in the spray solutions. This behavior can be explained when one considers that self-assembled species such as the squares exist in solution within an optimal concentration regime which is limited to the lower end by the so-called lowest self-assembly concentration (LSAC) [12]. To the upper end, polymer formation limits the concentration range. Consequently, relatively high concentrations compared to the ones typically used for ESI are needed for an efficient ionization of the squares under study here.

The corresponding ESI-FTICR mass spectra mostly consist of a series of differently charged self-assembled squares (Fig. 1). The almost exclusive observation of 4:4 complexes is a strong indication that the squares present in solution are transferred into the gas phase as intact macrocycles. The series of signals is caused by stripping off triflate counter ions from the squares. The observed signals range from the loss of two triflates giving rise to [**1a**–2TfO]$^{2+}$ up to the sevenfold charged square [**1a**–7TfO]$^{7+}$. While the experimental isotope patterns for the 3+ and 5+ charge states closely match those calculated on the basis of natural abundances, the doubly and quadruply charged ions are superimposed by a minor amount of singly and doubly charged fragments, respectively. The doubly charged square is also superimposed by some quadruply charged species which might be assigned to dimers of squares [11]. The small amount of doubly charged triangle [**1b**–2TfO]$^{2+}$ is due to the gas-phase fragmentation of [**1a**–3TfO]$^{3+}$ (see below).

Supramolecular squares readily dissociate in the gas phase [11]. As stated above, fragmentation can be induced simply by choosing longer hexapole ion collection times. A major part of the observed ions then passes a longer timespan in the ion-collecting hexapole of the ESI source and fragments there. Another possibility is to set the capillary exit voltage to higher values and thus perform collision-induced dissociation in the second pumping stage of the ion source. In both cases, the spectra change significantly. Monomeric and dimeric species prevail. Further, "corner-rich" fragments seem to be more stable than complexes with more edges than corners. As an example, the 2:1 complex [(dppp)Pt]$_2$(bipy)(TfO)$_3^+$ is a typical product after longer hexapole times, whereas the 2:2 complex [(dppp)Pt]$_2$(bipy)$_2$(TfO)$_3^+$ with an additional

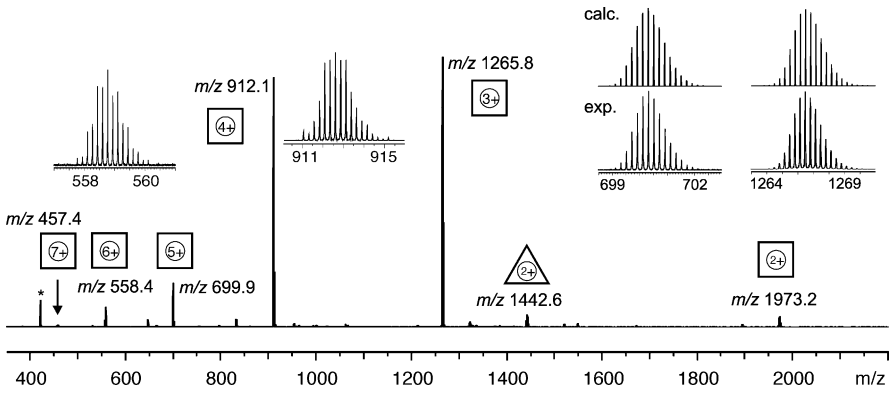

Fig. 1. Positive-mode ESI mass spectrum of the squares **1a** under very soft ionization conditions. The indicated *m/z* values refer to ^{195}Pt. Peaks due to electronic noise are marked with an asterisk.

bipyridine edge ligand is less stable and a 2:3 complex is not observed at all. Similarly, the "naked" corner (dppp)Pt(TfO)$^+$ is one of the major final fragmentation products. The 1:1 complex (dppp)Pt(bipy)(TfO)$^+$ with one bipyridine ligand is often detected, but easily loses the bipyridine ligand, whereas a singly charged 1:2 complex (dppp)Pt(bipy)$_2$(TfO)$^+$ with two bipyridine ligands is not observed at all.

Note that for all complexes with equal numbers of corners and edges [(dppp)Pt(bipy)]$_n$(TfO)$_{2n-m}^{m+}$ with $n > 2$, two structural possibilities exist, a macrocycle and an open chain. Despite of this ambiguity, we sometimes speak of triangles and squares in the following instead of 3:3 and 4:4 complexes, respectively, for the sake of simplicity. The most stable isomer at least for the 3:3 and 4:4 complexes surely is the cyclic one because it contains one additional Pt–N coordinative bond. The decision whether such a species in the gas phase is a cycle or an open chain is difficult to make by mass spectrometric means. At first sight, an open chain should lose its terminal edge ligand, which is bound only on one side, more easily than a closed macrocyclic structure in which every edge ligand is coordinated to two metal corner pieces. But fragmentation of a cycle surely starts with cleavage of a coordinative Pt–N bond, a process directly leading to the corresponding open-chain structure and thus rendering detectable differences in the fragmentation patterns unlikely.

Before we discuss the dissociation behavior of the squares **1a** and triangles **1b**, we will have a closer look on the fragmentation pathways of the corresponding smaller mono- and dinuclear complexes. This approach facilitates a separation of primary and subsequent fragmentation pathways and thus the understanding of the more complicated aggregates.

The singly charged "naked" corner (dppp)Pt(TfO)$^+$ loses TfOH upon irradiation with the IR-laser (Fig. 2a) as the only primary fragmentation channel. At longer irradiation times, subsequent losses of H_2 start to occur. Expulsion of a radical TfO$^\bullet$ is not observed. The same behavior is also detected with other counter ions, i.e., (dppp)Pt(CN)$^+$ loses HCN. We have not tried to determine the exact deprotonation site which could be achieved by deuterium labeling. Yet, the same loss of TfOH from the respective complex (^{t}Bubipy)Pt(TfO)$^+$ (see below), which bears a completely different corner ligand, indicates that the energetically favored loss of a closed-shell neutral molecule instead of a radical is the driving force for the fragmentation. Obviously, the coordinatively unsaturated Pt ion mediates reactions within the ligand attached to it [11b].

The interpretation of the IRMPD spectra of the 1:1 complex (dppp)Pt(bipy)(TfO)$^+$ with one bipyridine ligand is straightforward (Fig. 2b): first, bipyridine is split off, then the expected loss of TfOH takes place. The amount of fragmentation is very large compared to the other compounds of this study under similar conditions. Thus, the binding of bipyridine is comparatively weak in this complex. Also, the Pt(II) corner is coordinatively saturated by the bidentated dppp, the bipyridine, and the triflate counter ion and thus it is unlikely that it mediates the same C–H bond activation reactions seen before.

The smallest singly charged dinuclear complex [(dppp)Pt]$_2$(bipy)(TfO)$_3^+$ shows two major primary fragmentation channels (Fig. 2c). The first one includes the loss of a neutral corner piece (dppp)Pt(TfO)$_2$ and results in the monomeric mono-bipyridine 1:1 complex (dppp)Pt(bipy)(TfO)$^+$ discussed just above. As expected, this ion subsequently loses bipyridine and TfOH. Despite the clear prevalence of such a subsequent ligand expulsion, a small amount of direct loss of a neutral corner-bipyridine complex (dppp)Pt(bipy)(TfO)$_2$ cannot be ruled out completely. The second major fragmentation pathway is an unexpected one: the bipyridine edge is lost without separation of the two metal corner complexes. The two corner pieces in the resulting ion are no longer tied together by quasi-covalent Pt–N bonds. The two positively charged metal corners consequently must be bridged by at least two of the three TfO$^-$ anions instead in order to compensate for charge repulsion. This fact may also indicate that the anions do not simply play spectator roles in the other gas-phase adduct complexes either. For example, the three counter ions might play a major role to tie the two charged corners pieces together also in the 2:1 complex [(dppp)Pt]$_2$(bipy)(TfO)$_3^+$.

Finally, the fragmentation of the 2:2 complex [(dppp)Pt(bipy)]$_2$(TfO)$_3^+$ starts with a loss of the terminal bypiridine (Fig. 2d) yielding the dinuclear 2:1 complex just discussed, which is confirmed by identical subsequent fragmentation pathways.

The next step towards more complex ions would be a 3:2 complex with three corners connected by two bipyridine edges. However, such a complex (singly, doubly or triply charged) is

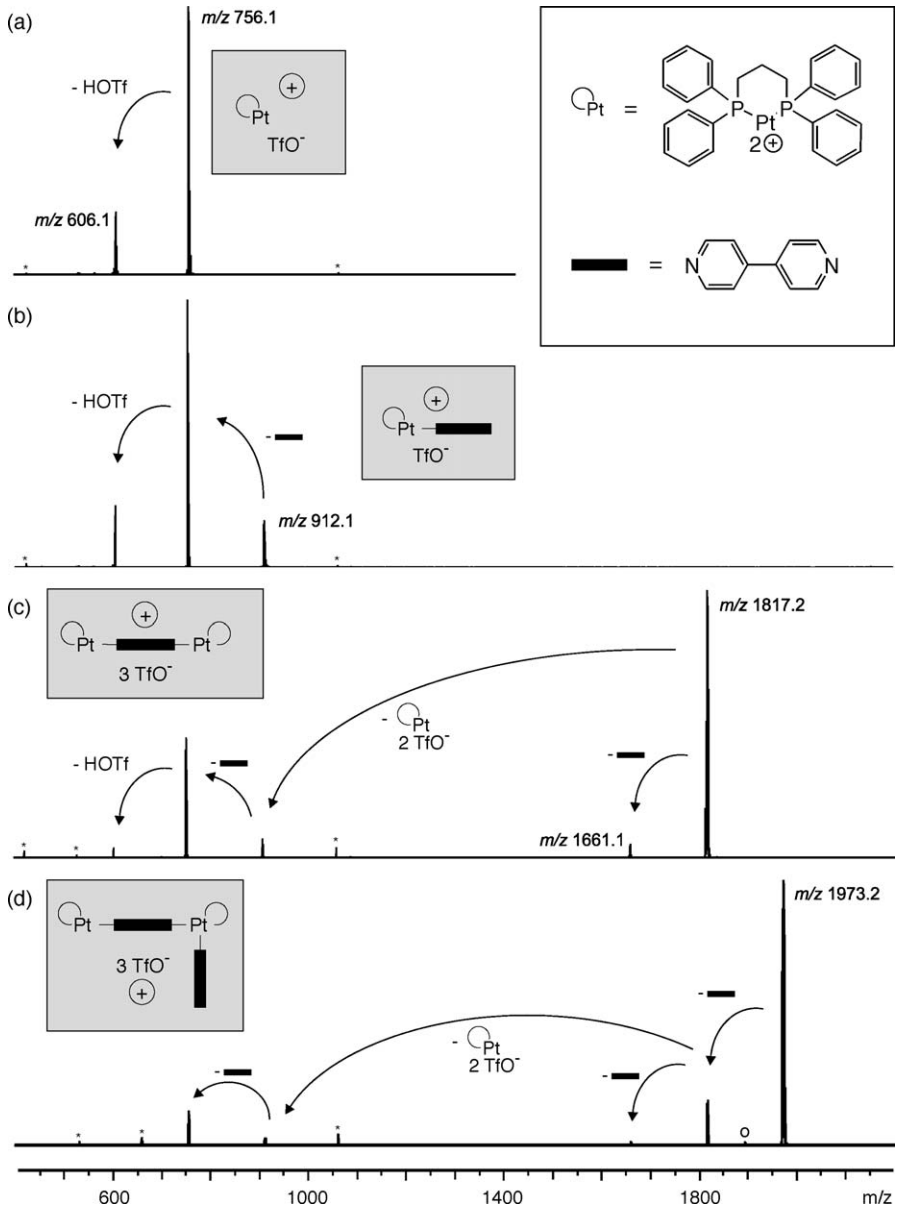

Fig. 2. IRMPD MS/MS spectra of the denoted mass-selected fragments of **1** (0.2 s irradiation time at 22.5 W laser power). The indicated *m*/*z* values refer to ^{195}Pt. Peaks due to electronic noise are marked with an asterisk. The open circle in (d) marks an ion which stems from bipyridine loss from a small amount of doubly charged square [**1a**–2TfO]$^{2+}$ which has the same *m*/*z* value as the desired singly charged 2:2 complex and therefore is still present after mass-selection.

not visible in the ESI mass spectra of **1a** in abundances sufficient for MS/MS experiments. Nevertheless, it can be generated from singly charged triangles [**1b**–TfO]$^+$ through a loss of bipyridine during IRMPD (Fig. 3a). The process is followed again by a loss of a second bipyridine.

Consecutive bipyridine losses are the only way of fragmentation for the singly charged 3:3 complex [**1b**–TfO]$^+$ (Fig. 3a). A trace of "naked" edge (dppp)Pt(TfO)$^+$ is detected as well, which may be formed via expulsion of a neutral 2:1 complex [(dppp)Pt]$_2$(bipy)(TfO)$_4$ from the 3:1 complex produced by double bipyridine loss.

In contrast, bipyridine loss is one, but not the only fragmentation pathway for the doubly charged 3:3 complex [**1b**–2TfO]$^{2+}$ (Fig. 3b). In addition, fission into two singly charged fragments occurs, the 1:1 and the 2:2 complexes described above. The subsequent fragmentations exactly match the ones observed separately (Fig. 2b and d, respectively). The repulsive force between the two charges in [**1b**–2TfO]$^{2+}$ obviously favors a dissociation into two singly charged fragments. Thus, the charge state of the triangular adduct complex determines its fragmentation pattern.

The IRMPD spectra of the doubly charged open chain 4:3 complex (Fig. 4a) very much resemble the ones just discussed for the doubly charged triangle [**1b**–2TfO]$^{2+}$. Apart from loss of a bipyridine ligand, charge separation into the mononuclear complex (dppp)Pt(bipy)(TfO)$^+$ and a 3:2 complex (the rest of the chain) is observed. The hypothetical alternative of dissociation into a 2:2 and a 2:1 complex does not take place. The only difference to the doubly charged 3:3 complex (Fig. 3b) is the presence of the fourth edge, but this does not alter the fragmentation pathways.

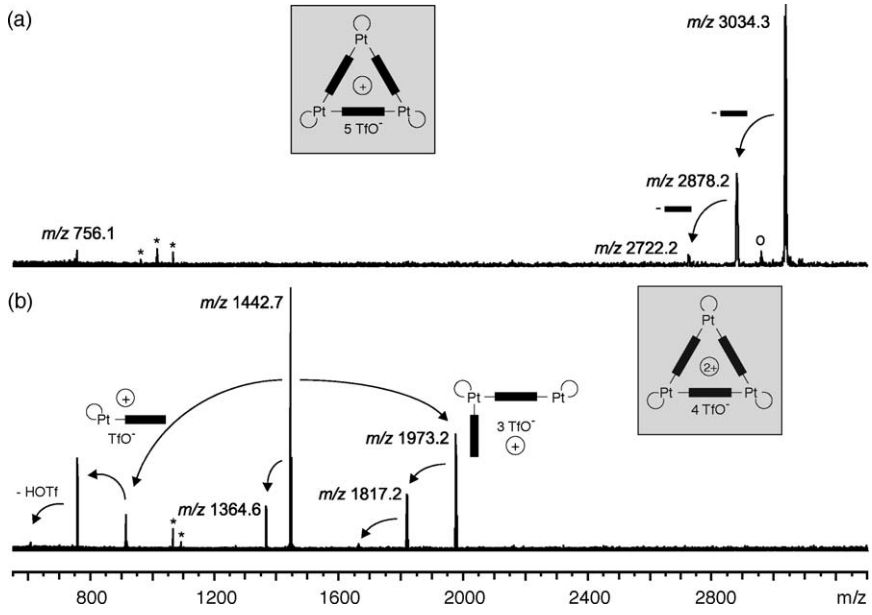

Fig. 3. IRMPD MS/MS spectra of (a) the mass-selected singly charged triangle [**1b**–TfO]$^{+}$ and (b) its doubly charged congener [**1b**–2TfO]$^{2+}$ (0.2 s irradiation time at 22.5 W laser power). The indicated *m/z* values refer to ^{195}Pt. Peaks due to electronic noise are marked with an asterisk. The open circle in (a) marks an ion which stems from bipyridine loss from a small amount of a doubly charged dimer [2 × **1b**–2TfO]$^{2+}$ which has the same *m/z* value as the desired singly charged 3:3 complex and therefore is still present after mass-selection. An unmarked arrow in (b) stands for loss of a bipyridine ligand.

Interestingly, the intact doubly charged 4:4 complex [**1a**–2TfO]$^{2+}$ does not undergo a direct charge separation step (Fig. 4b and Scheme 2). Loss of bipyridine is the only primary fragmentation channel we observed [13]. At longer irradiation times, the corner (dppp)Pt(TfO)$^{+}$ and the singly charged 3:2 complex are also detected; yet, it is very probable that they are the result of further fragmentation of the initially formed 4:3 complex (see Fig. 4a). The striking difference between the doubly charged triangle and the doubly charged square can be explained by size arguments. In a triangle, the two charges can be distributed over two adjacent corners separating them by one bipyridine ligand which translates into a metal–metal distance of ca. 1.1 nm [14]. In a square, however, the two charges can be located at diagonally opposed corners, increasing their distance to more than 1.5 nm and thus diminishing charge repulsion. Consequently, the doubly charged square fragments in close analogy to the singly charged triangle rather than its doubly charged analogue.

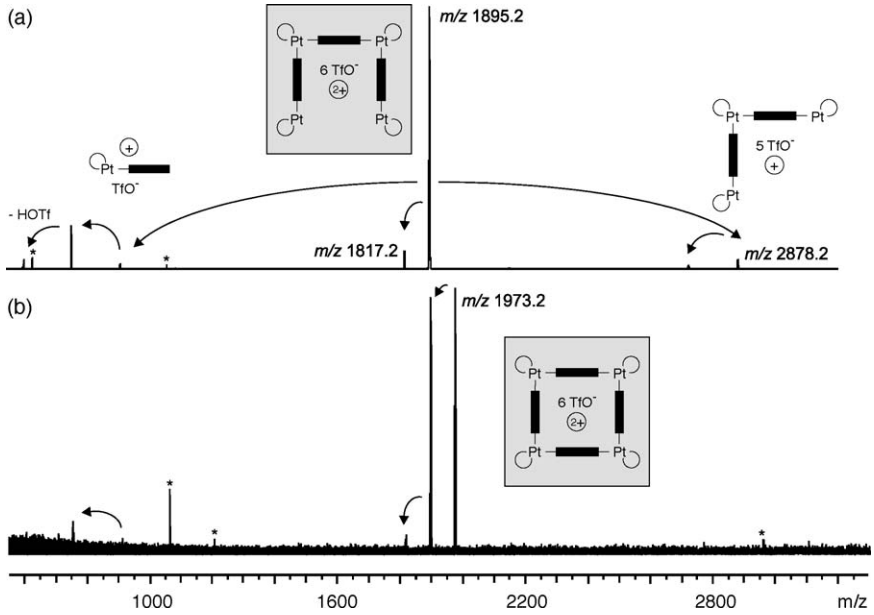

Fig. 4. IRMPD MS/MS spectra of (a) the mass-selected 4:3 complex of **1** (0.5 s irradiation time at 22.5 W laser power) and (b) the doubly charged square [**1a**–2TfO]$^{2+}$ (0.1 s irradiation time at 12.5 W laser power). The indicated *m/z* values refer to ^{195}Pt. Peaks due to electronic noise are marked with an asterisk. An unmarked arrow stands for loss of a bipyridine ligand [13].

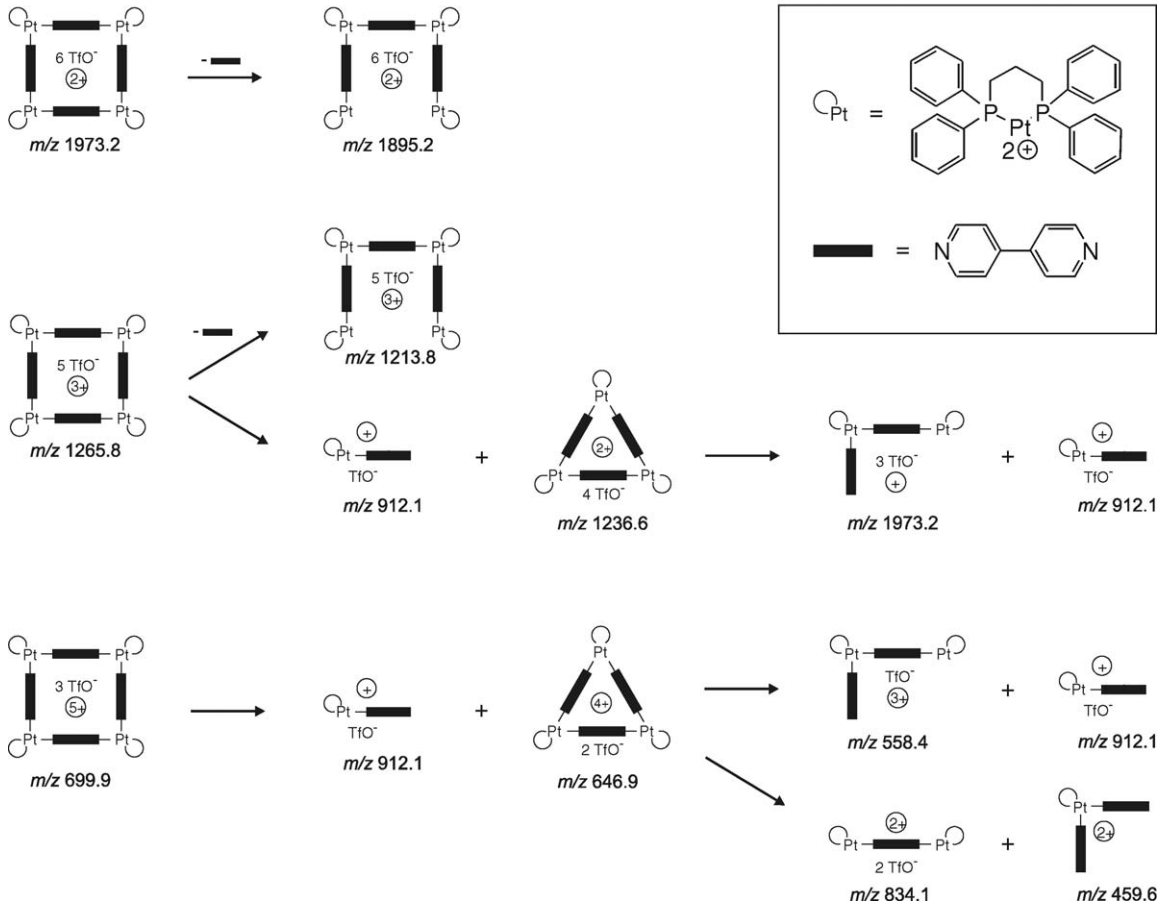

Scheme 2.

Based on these assumptions, the fragmentation behavior changes as expected for more highly charged squares. The triply charged 4:4 complex [**1a**–3TfO]$^{3+}$ not only looses one bypridine, but also exhibits fragmentation under charge separation leading to the singly charged monomeric 1:1 complex (dppp)Pt(bipy)(TfO)$^{+}$ and a doubly charged 3:3 complex [**1b**–2TfO]$^{2+}$ (Scheme 2) [11]. It is interesting to note that only one out of several possible charge separation reactions occurs. No dissociation into two square halves, one singly, one doubly charged is observed. Instead, only the dissociation into singly charged 1:1 and doubly charged 3:3 complexes is found as primary process. Two reasons may account for this finding: (a) if we assume that a larger species can more easily accommodate two charges than a smaller ion (as observed above for the doubly charged triangle and square), the fragmentation into a 1:1 and a 3:3 complex seems to yield the energetically more favorable ions. (b) The second possibility is a ring opening reaction followed by a backside [15] attack as shown in Scheme 3. The new Pt–N bond which closes the triangle is formed at the same time as the singly charged 1:1 complex is lost and thus may provide a substantial reduction of the barrier for this process. In contrast, no such backside attack is possible for geometrical reasons for the generation of two halves of the square. Consequently, this reaction is less favorable in energy and thus cannot efficiently compete with the formation of 1:1 and 3:3 complexes.

Quadruply charged squares [**1a**–4TfO]$^{4+}$ are detected in the ESI spectra (Fig. 1) with quite high abundance. However, they are superimposed with fragments appearing at the same *m*/*z* ratio. This causes problems with the mass-selection of the quadruply charged 4:4 complex in MS/MS experiments. Another problem is that two possible products, i.e., the doubly charged 2:2 complex and the singly charged 1:1 complex both appear at the same *m*/*z* ratio as the parent ion. Consequently, we refrain from a discussion of the dissociation pathways of the quadruply charged squares.

The dissociation of the 5+ charge state [**1a**–5TfO]$^{5+}$ (Fig. 5 and Scheme 2) can however be analyzed, although the abundance of this ion is already quite low. First of all, the typical loss of a bypiridine ligand, which would lead to a 4:3 complex in its 5+ charge state, is not observed at all. Secondly, fragmentation into a singly charged mononuclear 1:1 complex (dppp)Pt(bipy)(TfO)$^{+}$ and a quadruply charged 3:3 complex [**1b**–4TfO]$^{4+}$ is the major primary fragmentation pathway, in close analogy to the behavior of the triply charged square [**1a**–3TfO]$^{3+}$. Again, no dissociation into two halves is observed. While the triply charged 2:2 complex of corner and bipyridine is observed at *m*/*z* 558.4, its doubly charged counterpart is not seen in the MS/MS spectrum; the isotopic pattern at *m*/*z* 912.1 does not show any indications for a superposition with a doubly charged species. The ion at *m*/*z* 558.4 and all other decomposition products can easily be

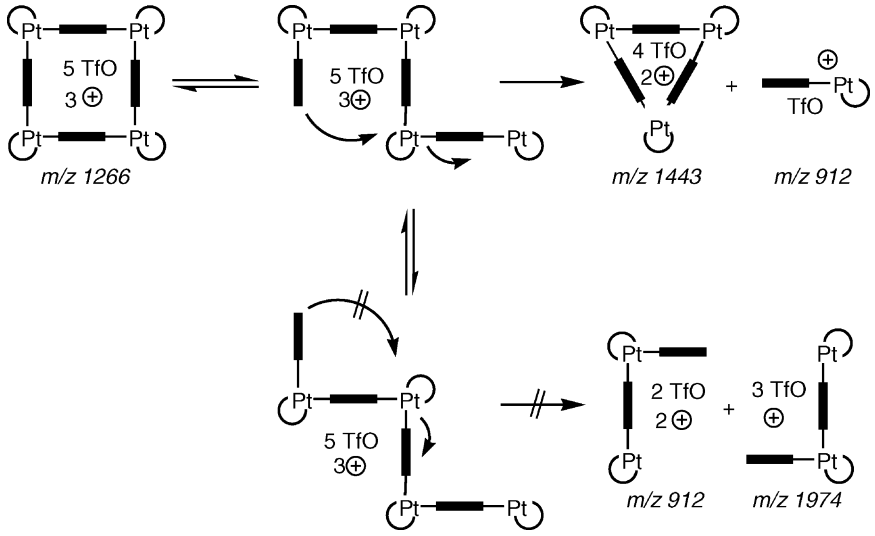

Scheme 3.

interpreted as secondary fragments stemming from the quadruply charged triangle (Scheme 2). Two pairs of complementary fragmentation products are observed. This finding is important with respect to the question whether the formation of triangles in the gas phase proceeds through neighbor group participation as discussed above (Scheme 3). If the charges would just be distributed according to the sizes of the ions, it is not clear, why the primary channel leads to a 1+/4+ fragmentation, while no 2+/3+ separation of charges is observed, while such competing channels are nicely seen for the quadruply charged triangle. In contrast, if a backside attack mechanism is indeed operative, it becomes clear why the quadruply charged triangle wins the competition with other channels. The fragmentation reactions of the 5+ charge state of the square thus nicely support this backside attack mechanism.

The IRMPD experiments reported so far make clear that the charge state of the self-assembled complex has a significant effect on the fragmentation behavior. The higher the charge, the easier the fragmentation and the larger the number of dissociation products.

In addition, also the structural details of the corner and edge ligands determine the fragmentation patterns. Thus, square **2a** [9d,e] built from elongated bipyridine edge ligands and ^{t}butyl-substituted bipyridine (^{t}Bubipy) Pt-complexes at the corners (Fig. 6) has been chosen for comparison. Irradiation of the mass-selected triply charged 4:4 complex [**2a**–3TfO]$^{3+}$ shows the loss of an edge ligand, but formation of a 3:3 complex is not observed at all (Fig. 6). Instead, a singly charged 2:1 complex is observed in addition to the expected 1:1 complex. As doubly charged triangles [**2b**–2TfO]$^{2+}$ are present in the normal ESI

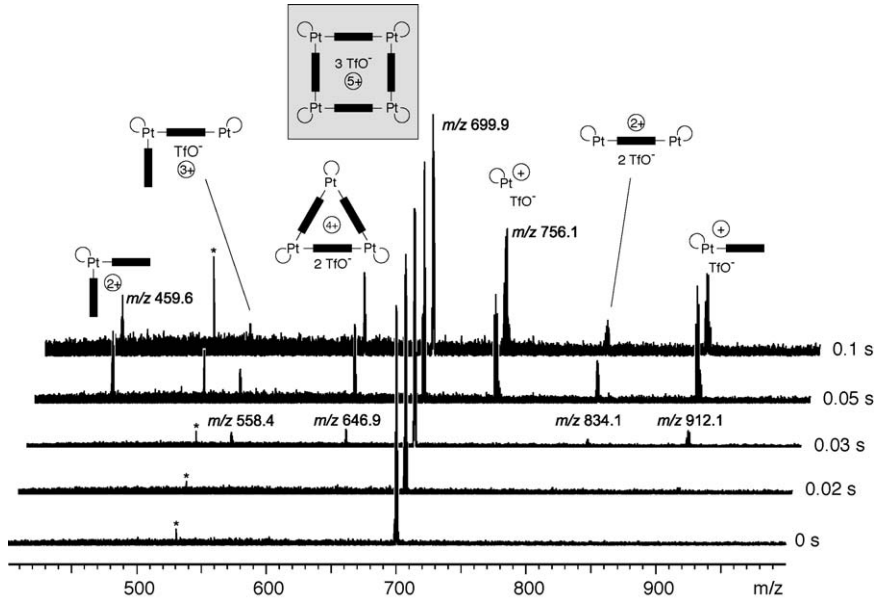

Fig. 5. IRMPD MS/MS spectra of the mass-selected squares [**1a**–5TfO]$^{5+}$ with the indicated irradiation times at 6.25 W (0.02 and 0.03 s) and 12.5 W (0.05 and 0.1 s) laser power. The indicated *m*/*z* values refer to ^{195}Pt. Peaks due to electronic noise are marked with an asterisk.

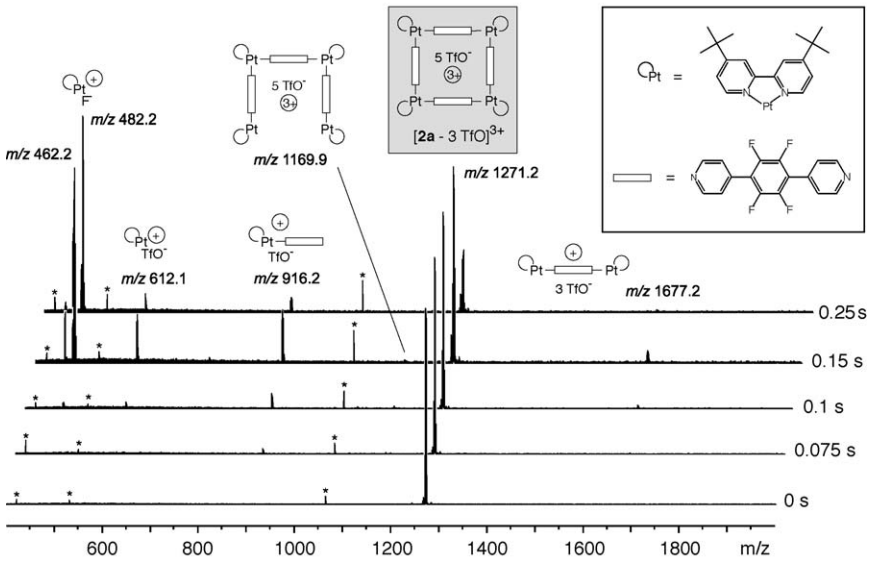

Fig. 6. IRMPD MS/MS spectra of the mass-selected squares [**2a**–3TfO]$^{3+}$ with the indicated irradiation times at 20 W laser power. The indicated *m*/*z* values refer to ^{195}Pt. Peaks due to electronic noise are marked with an asterisk.

spectra of a solution of **2**, they should be stable enough to be detected as intermediates during fragmentation of the squares. Thus, we conclude that other dissociation pathways are preferred. The fragmentation mechanism derived for [**1a**–3TfO]$^{3+}$ therefore cannot be assigned to any given triply charged metallosupramolecular square, even though the topology of the species and even the corner metal may be the same.

We note in passing that another difference to the Stang-type squares **1a** appears in the lower mass range of the spectra. The consecutive fragmentation of the corner (^{t}Bubipy)Pt(TfO)$^+$ does not only involve the expected loss of TfOH, but also the formation of (^{t}Bubipy)Pt(F)$^+$. A similar C–F bond activation in the triflate anion is not observed for the corresponding corner (dppp)Pt(TfO)$^+$. The reason may be found in different electronic properties at the metal core induced by different electron donor capacities of the P and N chelate ligands, respectively.

4. Conclusions

A first general observation in the experiments is the ubiquitous loss of bipyridine edge ligands from almost any complex discussed here. It even occurs from dinuclear 2:1 complexes like [(dppp)Pt]$_2$(bipy)(TfO)$_3^+$ in which the bypiridine likely serves as a linker between the two metal corners. In this case, the product ion [(dppp)Pt]$_2$(TfO)$_3^+$ has to be held together by anions bridging the metal centers. In accordance with this first observation is a second one: complexes with more corners than edges seem to be significantly more stable than the edge-rich types.

The charge state of polynuclear complexes significantly affects the fragmentation pattern. Thus, bipyridine losses prevail for the doubly charged square [**1b**–2TfO]$^{2+}$, whereas dissociation in two or even more charged metal complexes gains importance for higher charged species due to enhanced Coulomb repulsion. A charge separation pathway occurs already at the 2+ state for the triangles, but needs at least three charges for the squares. Nevertheless, the structure and electronic properties of the building blocks of the self-assembled aggregates also determine the fragmentation patterns, even though the topology of squares may be the same.

The most interesting conclusion from our study is the backside attack mechanism leading to a preference of the dissociation of squares into 1:1 and 3:3 complexes even for the 5+ charge state. This mechanism can be interpreted as a supramolecular analogue of classical neighbor group effects well known in organic chemistry. The implications of such a mechanism are: (a) even for bipyridine as the edges, the formation of triangles is possible, although they are not detected in solution for example by NMR experiments. (b) If triangles can be formed, their strain energy must be lower than the bond dissociation energy of one Pt–N bond. Otherwise, a backside attack mechanism would not reduce the barrier for fragmentation significantly and one would expect to observe a competition between different mechanisms as observed for the quadruply charged triangle. Since the exchange of subunits in solution makes the detection of such a mechanism in the condensed phase impossible, the gas phase permits a detailed mechanistic analysis and thus underlines the importance of gas-phase studies on supramolecular, non-covalently bound species.

Acknowledgments

We thank the Deutsche Forschungsgemeinschaft (DFG) and the Fonds der Chemischen Industrie (FCI) for financial support. A.R. thanks the Studienstiftung des Deutschen Volkes for support with a scholarship. C.A.S. is grateful for a Heisenberg fellowship of the DFG and a Dozentenstipendium from the FCI.

References

[1] (a) J.S. Lindsey, New J. Chem. 15 (1991) 153;
(b) G.M. Whitesides, J.P. Mathias, C.T. Seto, Science 254 (1991) 1312;

(c) D. Philp, J.F. Stoddart, Angew. Chem. 108 (1996) 1243;
D. Philp, J.F. Stoddart, Angew. Chem. Int. Ed. 35 (1996) 1154;
(d) C.A. Schalley, A. Lützen, M. Albrecht, Chem. Eur. J. 10 (2004) 1072.

[2] For selected reviews on polynuclear, self-assembling metal complexes, see;
(a) M. Fujita, in: J.L. Atwood, J.E.D. Davies, D.D. MacNicol, F. Vögtle, J.-M. Lehn, J.-P. Sauvage, M.W. Hosseini (Eds.), Comprehensive Supramolecular Chemistry, vol. 9, Pergamon, Oxford, 1996, p. 253;
(b) J.R. Fredericks, A.D. Hamilton, in: A.D. Hamilton (Ed.), Supramolecular Control of Structure and Reactivity—Perspectives in Supramolecular Chemistry, vol. 3, Wiley, New York, 1996, p. 1;
(c) M. Fujita, K. Ogura, Coord. Chem. Rev. 148 (1996) 249;
(d) M. Fujita, K. Ogura, Bull. Chem. Soc. Jpn. 69 (1996) 1471;
(e) C. Piguet, G. Bernardinelli, G. Hopfgartner, Chem. Rev. 97 (1997) 2005;
(f) P.J. Stang, B. Olenyuk, Acc. Chem. Res. 30 (1997) 502;
(g) M. Albrecht, Chem. Soc. Rev. 27 (1998) 281;
(h) C.J. Jones, Chem. Soc. Rev. 27 (1998) 289;
(i) M. Fujita, Chem. Soc. Rev. 27 (1998) 417;
(j) C. Piguet, J. Inclusion Phenom. Macrocyc. Chem. 34 (1999) 361;
(k) D.L. Caulder, K.N. Raymond, Acc. Chem. Res. 32 (1999) 975;
(l) S. Leininger, B. Olenyuk, P.J. Stang, Chem. Rev. 100 (2000) 853;
(m) M. Fujita, K. Umemoto, M. Yoshizawa, N. Fujita, T. Kusukawa, K. Biradha, Chem. Commun. (2001) 509;
(n) B.J. Holliday, C.A. Mirkin, Angew. Chem. 113 (2001) 2076;
B.J. Holliday, C.A. Mirkin, Angew. Chem. Int. Ed. 40 (2001) 2022;
(o) M. Albrecht, Chem. Rev. 101 (2001) 3457;
(p) D.W. Johnson, K.N. Raymond, Supramol. Chem. 13 (2001) 639;
(q) G.F. Swiegers, T.J. Malfetse, J. Inclusion Phenom. Macrocyc. Chem. 40 (2001) 253;
(r) F.A. Cotton, C. Lin, C.A. Murillo, Acc. Chem. Res. 34 (2001) 759.

[3] For reviews on the application of mass spectrometry to different aspects in host–guest and supramolecular chemistry, see;
(a) M. Vincenti, J. Mass Spectrom. 30 (1995) 925;
(b) J.S. Brodbelt, D.V. Dearden, in: J.L. Atwood, J.E.D. Davies, D.D. MacNicol, F. Vögtle, J.-M. Lehn, J.A. Ripmeester (Eds.), Comprehensive Supramolecular Chemistry, vol. 8, Pergamon, Oxford, 1996, p. 567;
(c) M. Przybylski, M.O. Glocker, Angew. Chem. 108 (1996) 878;
M. Przybylski, M.O. Glocker, Angew. Chem. Int. Ed. 35 (1996) 806;
(d) J.S. Brodbelt, Int. J. Mass Spectrom. 200 (2000) 57;
(e) C.A. Schalley, Int. J. Mass Spectrom. 194 (2000) 11;
(f) C.B. Lebrilla, Acc. Chem. Res. 34 (2001) 653;
(g) C.A. Schalley, Mass Spectrom. Rev. 20 (2001) 253.

[4] (a) J.A. Whiteford, E.M. Rachlin, P.J. Stang, Angew. Chem. 108 (1996) 2643;
J.A. Whiteford, E.M. Rachlin, P.J. Stang, Angew. Chem. Int. Ed. 35 (1996) 2524;
(b) S.M. Woessner, J.B. Helms, J.F. Houlis, B.P. Sullivan, Inorg. Chem. 38 (1999) 4380.

[5] (a) P.J. Stang, D.H. Cao, K. Chen, G.M. Gray, D.C. Muddiman, R.D. Smith, J. Am. Chem. Soc. 119 (1997) 5163;
(b) J. Manna, C.J. Kuehl, J.A. Whiteford, P.J. Stang, D.C. Muddiman, S.A. Hofstadler, R.D. Smith, J. Am. Chem. Soc. 119 (1997) 11611;
for a few examples of other species, such as cages and helicates, see;
(c) E. Leize, A. Van Dorsselaer, R. Krämer, J.-M. Lehn, J. Chem. Soc., Chem. Commun. (1993) 990;
(d) G. Hopfgartner, C. Piguet, J.D. Henion, J. Am. Soc. Mass Spectrom. 5 (1994) 748;
(e) A. Marquis-Rigault, A. Dupont-Gervais, A. Van Dorsselaer, J.-M. Lehn, Chem. Eur. J. 2 (1996) 1395;
(f) F.M. Romero, R. Ziessel, A. Dupont-Gervais, A. Van Dorsselaer, Chem. Commun. (1996) 551;
(g) A. Marquis-Rigault, A. Dupont-Gervais, P.N.W. Baxter, A. Van Dorsselaer, J.-M. Lehn, Inorg. Chem. 35 (1996) 2307;
(h) S. König, C. Brückner, K.N. Raymond, J.A. Leary, J. Am. Soc. Mass Spectrom. 9 (1998) 1099;
(i) G. Hopfgartner, F. Vilbois, C. Piguet, Rap. Commun. Mass Spectrom. 13 (1999) 302;
(j) M. Ziegler, J.J. Miranda, U.N. Andersen, D.W. Johnson, J.A. Leary, K.N. Raymond, Angew. Chem. 113 (2001) 755;
M. Ziegler, J.J. Miranda, U.N. Andersen, D.W. Johnson, J.A. Leary, K.N. Raymond, Angew. Chem. Int. Ed. 40 (2001) 733.

[6] S. Sakamoto, M. Fujita, K. Kim, K. Yamaguchi, Tetrahedron 56 (2000) 955 (besides the literature cited above dealing with squares, this article contains more MS references on capsules and other supramolecular species).

[7] (a) P.J. Stang, D.H. Cao, J. Am. Chem. Soc. 116 (1994) 4981;
(b) P.J. Stang, J.A. Whiteford, Organometallics 13 (1994) 3776;
(c) P.J. Stang, D.H. Cao, S. Saito, A.M. Arif, J. Am. Chem. Soc. 117 (1995) 6273;
(d) B. Olenyuk, J.A. Whiteford, P.J. Stang, J. Am. Chem. Soc. 118 (1996) 8221;
(e) F. Würthner, A. Sautter, Chem. Commun. (2000) 445;
(f) F. Würthner, A. Sautter, D. Schmid, P.J.A. Weber, Chem. Eur. J. 7 (2001) 894.

[8] (a) M. Fujita, J. Yazaki, K. Ogura, J. Am. Chem. Soc. 112 (1990) 5645;
(b) R.V. Slone, D.I. Yoon, R.M. Calburn, J.T. Hupp, J. Am. Chem. Soc. 117 (1995) 11813;
(c) R.V. Slone, J.T. Hupp, C.L. Stern, T.E. Albrecht-Schmitt, Inorg. Chem. 35 (1996) 4096;
(d) M. Fujita, O. Sasaki, T. Mitsuhashi, T. Fujita, J. Yazaki, K. Yamaguchi, K. Ogura, Chem. Commun. (1996) 1535;
(e) R.V. Slone, J.T. Hupp, Inorg. Chem. 36 (1997) 5422.

[9] For square-triangle equilibria, see;
(a) S.B. Lee, S. Hwang, D.S. Chung, H. Yun, J.-I. Hong, Tetrahedron Lett. 39 (1998) 873;
(b) R.-D. Schnebeck, E. Freisinger, B. Lippert, Eur. J. Org. Chem. (2000) 1193;
(c) A. Sautter, D.G. Schmid, G. Jung, F. Würthner, J. Am. Chem. Soc. 123 (2001) 5424;
(d) M. Ferrer, L. Rodríguez, O. Rossell, J. Organomet. Chem. 681 (2003) 158;
(e) M. Ferrer, M. Mounir, O. Rossell, E. Ruiz, M.A. Maestro, Inorg. Chem. 42 (2003) 5890.

[10] Examples of triangles;
(a) M. Fujita, M. Aoyagi, K. Ogura, Inorg. Chim. Acta 246 (1996) 53;
(b) R.-D. Schnebeck, L. Randaccio, E. Zangrando, B. Lippert, Angew. Chem. 110 (1998) 128;
R.-D. Schnebeck, L. Randaccio, E. Zangrando, B. Lippert, Angew. Chem. Int. Ed. 37 (1998) 119;
(c) R.-D. Schnebeck, E. Freisinger, B. Lippert, Chem. Commun. (1999) 675;
(d) S.-W. Lai, M.C.-W. Chan, S.-M. Peng, C.-M. Che, Angew. Chem. 111 (1999) 708;
S.-W. Lai, M.C.-W. Chan, S.-M. Peng, C.-M. Che, Angew. Chem. Int. Ed. 38 (1999) 669;
(e) T. Habereder, M. Warchhold, H. Nöth, K. Severin, Angew. Chem. 111 (1999) 3422;
T. Habereder, M. Warchhold, H. Nöth, K. Severin, Angew. Chem. Int. Ed. 38 (1999) 3225;
(f) S.-S. Sun, A.J. Lees, Inorg. Chem. 38 (1999) 4181;
(g) S.-S. Sun, A.J. Lees, J. Am. Chem. Soc. 122 (2000) 8956;
(h) R.-D. Schnebeck, E. Friesinger, F. Glahé, B. Lippert, J. Am. Chem. Soc. 122 (2000) 1381.

[11] (a) C.A. Schalley, T. Müller, P. Linnartz, M. Witt, M. Schäfer, A. Lützen, Chem. Eur. J. 8 (2002) 3538;
(b) K.S. Jeong, S.Y. Kim, U.-S. Shin, M. Kogej, N.T.M. Hai, P. Broekmann, N. Jeong, B. Kirchner, M. Reiher, C.A. Schalley, J. Am. Chem. Soc. 127 (2005) 17672–17685.

[12] (a) X. Chi, A.J. Guerin, R.A. Haycock, C.A. Hunter, L.D. Sarson, J. Chem. Soc., Chem. Commun. (1995) 2567;
(b) G. Ercolani, J. Phys. Chem. B 102 (1998) 5699.

[13] Note that the signal at *m*/*z* 1817 in Fig. 4b is a superposition of a doubly charged 4:2 complex as expected from double bipyridine loss from [**1a**–2 TfO]$^{2+}$ and a singly charged 2:1 complex. The latter stems from bipyri-

dine loss from a small amount of the singly charged 2:2 complex present underneath the isotopic pattern of the doubly charged square.

[14] (a) M. Aoyagi, K. Biradha, M. Fujita, Bull. Chem. Soc. Jpn. 72 (1999) 2603;
(b) C. Safarowsky, L. Merz, A. Rang, P. Broekmann, B.A. Hermann, C.A. Schalley, Angew. Chem. 116 (2004) 1311;
C. Safarowsky, L. Merz, A. Rang, P. Broekmann, B.A. Hermann, C.A. Schalley, Angew. Chem. Int. Ed. 43 (2004) 1291.

[15] The actual geometry of the attack is not known. The term "backside" here is simply used in analogy to the neighbour group effect known for S_N2 substitution reactions in organic chemistry.